SUPPLEMENTARY MATERIALS

SUPPLEMENTARY EXPERIMENTAL PROCEDURES

SEP Method 1. *Drosophila* Strains

Drosophila melanogaster w^{1118}, and *w*; T(2;3)* ap^{Xa}, ap^{Xa} */ CyO; TM3,* Sb^{1} (used for linkage group analysis) were obtained from the Bloomington Stock Center (Bloomington, IN). w^{1118} was used as host for generating the transgenic strains. w^{1118}*; P{*w^{+}*, Act88Ffln*$^{+}$*};* fln^{o}*, e*, the transgenic strain expressing the wild-type flightin gene in a fln^{0} background [1], was used as the control line and henceforth will be referred to as fln^{+}. The flightin null mutant line (fln^{0}) used here is described in [2]. All fly lines were maintained in a constant temperature and humidity (21±1°C, 70%) environmental room on a 12:12 light:dark cycle.

SEP Method 2. Construction of the Transformation Vector

The N-terminal 62 amino acids deletion was engineered in a P-element transformation vector pCaSpeR (Flybase ID: FBmc0000168) containing the full-length flightin gene and the actin *Act88F* promoter [1] by using primers:

Forward: 5' TTTTTGGTACCATGAAAGCACCGCCGCCTCCG 3' and

Reverse: 5' GCACTAGCTGCAGAACCCCTCATACCTGCCG 3' with underlined bases representing KpnI and PstI restriction enzyme sites in the forward and reverse primer sequences, respectively. The forward primer was designed to amplify starting at the 189th base of the coding sequence of the flightin gene and to introduce a new ATG start site and KpnI site in the overhang region. The reverse primer was the same as designed for the 3' end of the 1.14 kb flightin genomic fragment previously cloned into pCaSpeR [1].

The resulting 954 bp PCR product, deleted for the 62 amino acids after Methionine (see Figure S1), was cloned into a pCaSperR from which the 1.14 kb flightin gene was excised using KpnI and PstI restriction endonucleases. The same aforementioned primers were used for DNA sequencing verification of the N-terminal deleted construct.

SEP Method 3. Generation of the *P{fln$^{\Delta N62}$}* Strains

Microinjection of the transformation vector into w^{1118} host strain was carried out by Genetic Services, Inc., Sudbury, MA. Linkage group was determined by standard crosses to *w*; T(2;3) ap^{Xa}, ap^{Xa} / CyO; TM3, Sb^{1}*. Five parental strains were created in a *fln^{+}* background, each with a second chromosome insertion, and were subsequently crossed into the flightin null background (*fln^{0}*) [2] to generate homozygous transgenic strains with no endogenous flightin expression. All the transformed strains have the genotype w^{1118};*P{w^{+}, Act88Ffln$^{\Delta N62}$}*; *fln^{0}*, *e* and herein will be referred to as *fln$^{\Delta N62X}$* where X is a letter from A through E. Expression of the transgene was confirmed by RT- PCR analysis *via*. RNA isolated from 30 two-day old flies (data not shown), using the forward and reverse primers described in the previous section. Based on protein expression of the transgene and flight ability (see below), two lines, *fln$^{\Delta N62A}$* and *fln$^{\Delta N62B}$* were selected for subsequent analyses.

SEP Method 4. Gel Electrophoresis and Western Blot Analysis

One dimensional gel electrophoresis and western blot analysis were done as previously described [1], with the following modifications. Indirect flight muscle (IFM) fibers from three flies from each of the strains, i.e., the control *fln^{+}*, *fln^{0}* and N-terminal deletion lines were dissected in

skinning solution (pCa 8.0; 20 mM N,N-bis[2-hydroxyethyl]-2-aminoethanesulfonic acid (BES), 10 mM DTT, 5 mM EGTA, 1 mM Mg^{2+}, 5 mM MgATP, 0.25 mM P_i, protease inhibitor cocktail (Roche; Indianapolis, IN), ionic strength of 175 mEq adjusted with sodium methane sulfate, pH 7.0, 50% w/v glycerol, and 0.25% v/v Triton X-100.) and stored overnight at -20^{o}C in a fresh aliquot of the same skinning solution. The following morning the fibers were collected by a brief spin on a table top microfuge, the skinning solution was removed and the fibers rinsed five times for 3 minutes each in relaxing solution (pCa 8, 20 mM BES, 20 mM CP, 450 U/mL CPK, 1 mM DTT, 5 mM EGTA, 1 mM Mg^{2+}, 12 mM MgATP, 2 mM P_i, protease inhibitor cocktail, 200 mEq ionic strength, pH 7.0) to remove the glycerol and Triton X-100 completely. The fibers were then dissolved in SDS gel sample buffer (62.5 mM Tris-HCL, 100 mM DTT, 2% w/v SDS,and 20% w/v glycerol with protease inhibitor cocktail). 10 μL of each sample was loaded per lane of 10-20% gradient SDS-PAGE gels (Criterion Bio-Rad, Catalogue # 567-1114) in duplicate; one gel was stained with Krypton (Pierce, Rockford, IL) infrared protein stain and the other gel was blotted onto PVDF membrane (0.2 μm pore size, Bio-Rad Catalog # 162-0174) at 65V for 1 hr using a Tris-Glycine buffer (National Diagnostics, Atlanta, GA). For krypton staining, the gel was fixed with 50% v/v ethanol, 15% v/v acetic acid, stained overnight, destained with 5% v/v acetic acid, 0.1% v/v Tween-20 for 5 mins, and scanned in an Odyssey Imaging System (LI-COR Biosciences, Lincoln, NE). For western blots, PVDF membranes were blocked using a 1:1 Aquablock-PBS solution (Aquablock: East Coast Biologics, North Berwick, ME) and incubated with a 1:3000 dilution of anti-flightin polyclonal antibody [2]. After primary antibody incubation, the membrane was washed two times for 5 mins each and then three times for 15 mins each with PBST (1X PBS with 0.1% Tween-20). The membrane was then incubated for one hour in a 1:7500 dilution of secondary antibody, Alexafluor 680 goat anti-rabbit IgG (Invitrogen, Carlsbad, CA). The membrane was washed again with PBST

two times for 5 mins each, and then three times for 10 mins each, and a final wash with 1X PBS (without Tween-20) two times for 20 mins each. The blot was allowed to dry overnight in the dark and then scanned in an Odyssey Imaging System.

SEP Method 5. Courtship Behavior Recording and Analysis

The single pair courtship song recordings were for 30 mins each [3] using males aged 3 days and females aged 24 hrs or less. For single-pair courtship behavioral assays using 3-5 days old virgin male and female, the courtship activities were video recorded until successful copulation, or longer (up to 30–50 minutes) in the absence of copulation [4]. Courtship competition using 3-5 days old virgin males and females were video recorded for 30–50 minutes or until successful copulation [4]. Courtship index or (CI) is the percent fraction of the total recording time the male displayed courtship behaviors (orienting, chasing, tapping, licking, singing, copulation attempts), and wing extension index or (WEI) is the percent fraction of the total recording time the male extends and vibrates a wing for singing [4,15,16]. Both indices are expressed as percentages. Other courtship song parameters measured in this study here with abbreviations are: sine song frequency (SSF), intrapulse frequency (IPF), cycles per pulse (CPP), pulse length (PL), interpulse interval (IPI), and pulse duty cycle (PDC). The recorded songs were digitized and analyzed using Goldwave v5.58 [5]. Representative song oscillograms were generated with Audacity 2.0 [http://audacity.sourceforge.net/].

SEP Method 6. Transmission Electron Microscopy

Sections were imaged at 8000x magnification, 1.426 nm pixel size. Images were analyzed using NIH ImageJ [6] and Metamorph Software (Molecular Devices, LLC, California, USA). Values reported for the myofibril area and myofibril area per fiber cross-section (Table I) were measured using Metamorph Software. All other measurements (Tables I and II) were performed in Image J. The distance between the thick filament planes, $d_{1,0}$ [7], was quantified using two-dimensional Fourier transform (FFT) power spectra from cross sectional images of the myofibrils that were windowed into boxes of 512 × 512 or 1024 × 1024 pixels (for detailed protocol and validation of this method see below SEP Methods 7 and 8, respectively). $d_{1,0}$ was obtained from the inverse of the product of the FFT space distances and pixel size. The inter-thick filament spacing was calculated as $2/\sqrt{3}$ multiplied by $d_{1,0}$ [7]. Structural regularity was quantified by processing the following structural information:

i) Resolution to which the filaments in the myofibrillar lattice diffract was determined by measuring the distance from the center of the Fourier transform to the farthest visible spot.

ii) The short range disorder of the filaments in the myofibrillar lattice was evaluated by calculating the sharpness of the diffraction spots. The spot sharpness was determined with Image J by transforming the FFT of the original myofibrillar cross-sectional image to polar coordinates and plotting the intensity profile across the reflection lines. The half-width and the height ($\log_{10}$) of the intensity peaks at the (1,0) plane were measured.

SEP Method 7. Detailed Procedure for Fourier Processing of EM Myofibrillar Cross-sections to Quantify Myofilament Lattice Spacing and Regularity

FFT processing of EM cross-sectional images:

All cross section images with same magnification were selected without contrast enhancement, brightness modification and/or changing image size. Full cross-section of a single myofibril was selected (Figure MS1 left) and copied to a new image with 512×512 or 1024×1024 pixel size to make sure only myofilaments are included in the image as shown below in the snapshot (Figure MS1 right).

Figure MS1

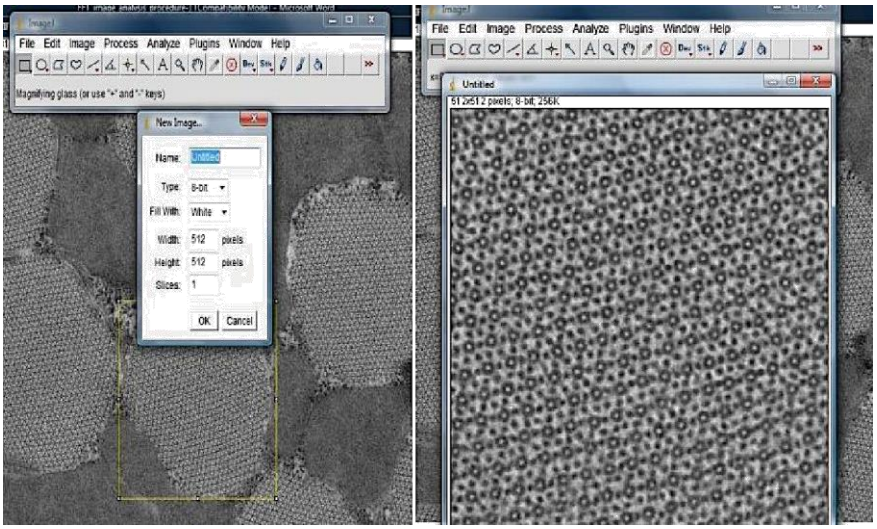

ImageJ FFT option was used to process the Fourier transform of the image as shown below (Figure MS2).

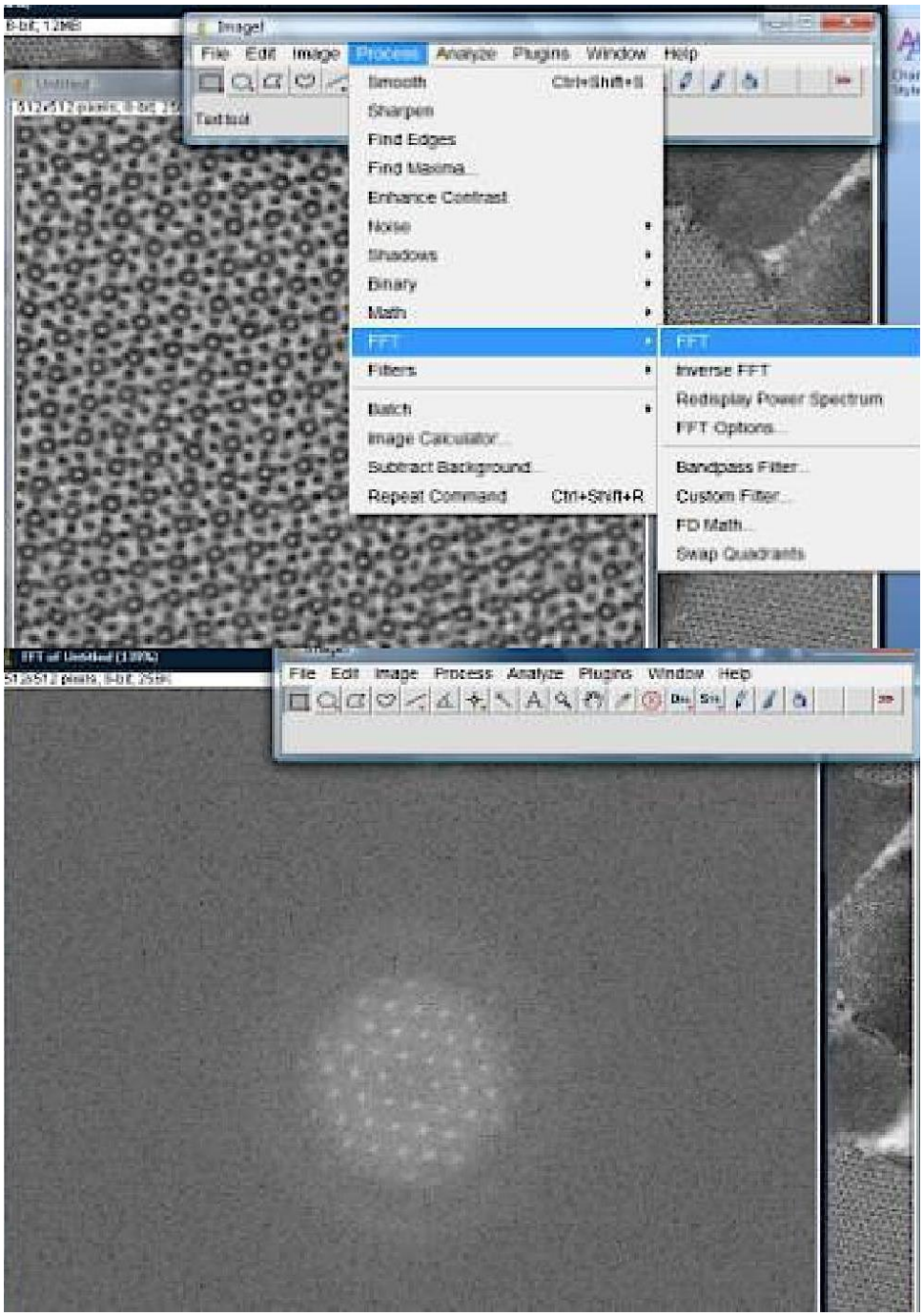

Figure MS2

FFT analysis to quantify inter-filament distance measurements:

Pixel size (eg.: 14.26Å) in the original EM image was noted down. FFT image was scaled (yellow horizontal line in figure MS3) arbitrarily as shown below in the snapshot (eg.: 512 pixels in length in Figure MS3).

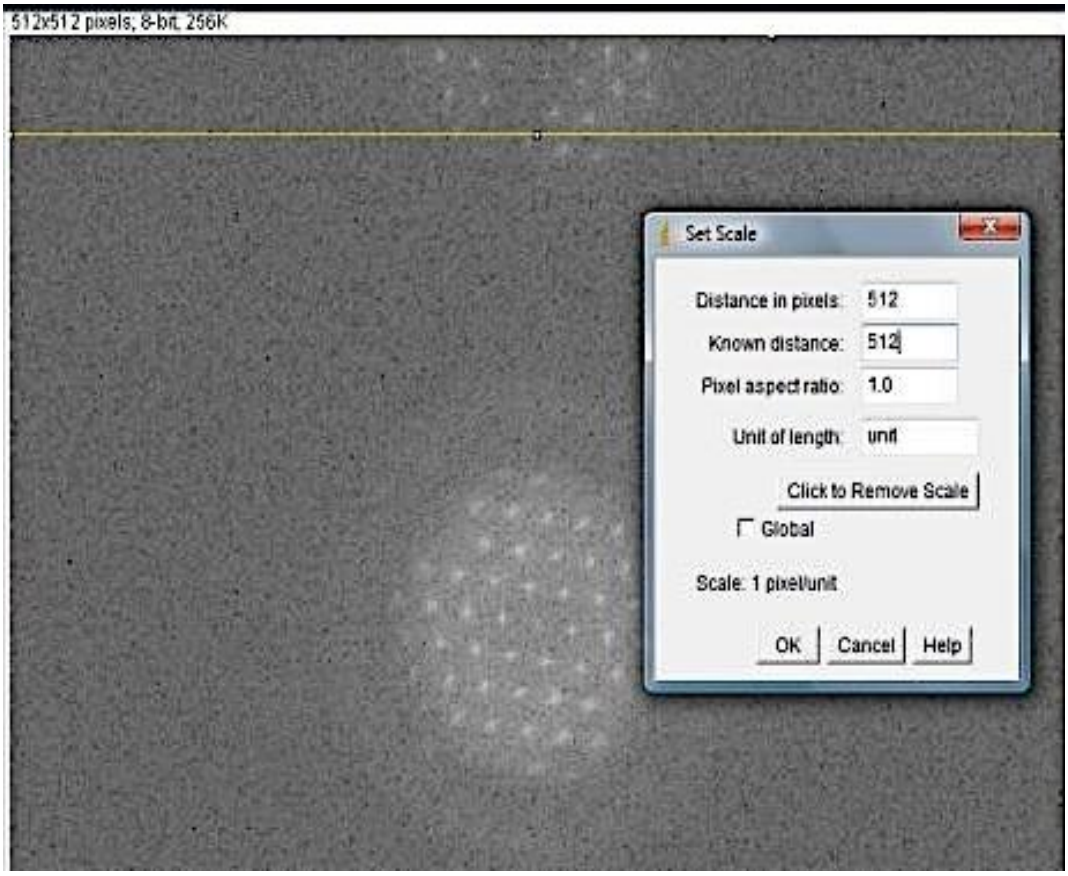

Figure MS3

The distance from the center to the 1st order reflection in the FFT was measured. For accuracy, the distance in pixels on a drawn line (passing through the center) was measured (Figure MS4) and was divided by the number of inter-spot distances included in the line. In this example (Figure MS4), the length of the line is 114.242 pixels and the number of spots passing through the line is seven. Thus, number of inter-spot distance = number of spots – 1= 7-1= 6 (in this example). The distance in pixels from the center to the 1st order reflection in the FFT = 114.242 / 6= 19.04 pixels.

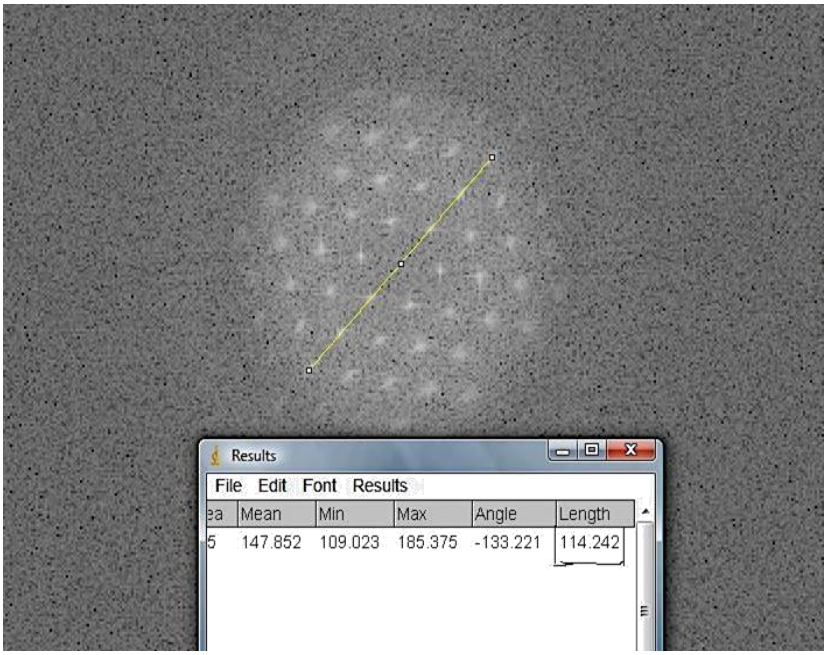

Figure MS4

There is a strict correlation between real and Fourier space. Total number of pixels of FFT × distance per pixel (from the original image) should be constant. Therefore, 512 × 14.26 Å = 19.04 × inter-filament distance ($d_{1,0}$).

Example: $d_{1,0}$ = 512 × 14.26 Å / 19.04 = 383.46 Å or 38.35 nm. Therefore, inter-thick filament distance = $2/\sqrt{3} \times d_{1,0}$ = 38.35 × $2/\sqrt{3}$ = 44.28 nm.

Order or regularity of the lattice as a measure of resolution of the Fourier power spectrum and the sharpness of the 1,0 FFT spot intensities:

Resolution:

FFT image was scaled. A line was drawn connecting as many spots as can be seen across both sides of the center of the FFT (Figure MS5). The distance in pixels of the line was measured and divided by 2 (eg. 138.593/2 spots= 69.3 pixel resolution in Fourier space). Resolution of the myofilament lattice was calculated as the total number of pixels of FFT × distance per pixel (from the original image) divided by pixel resolution in Fourier space. In this example, 512 × 1.426 nm / 69.3 = 10.54 nm resolution.

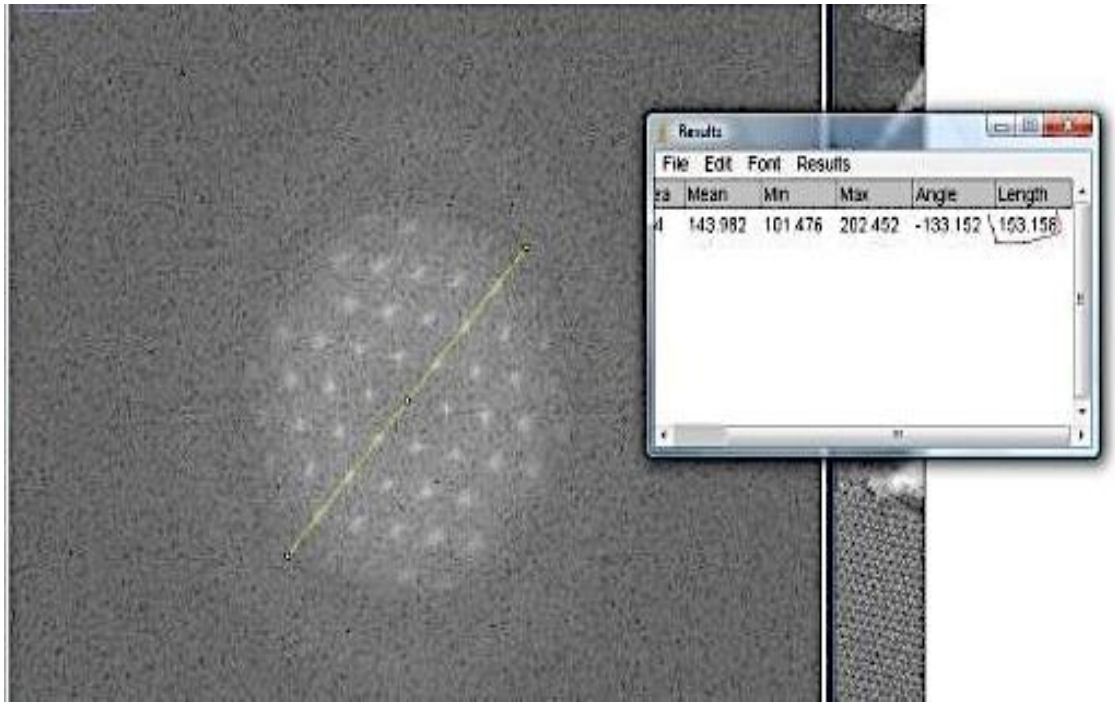

Figure MS5

Sharpness:

FFT images were transformed from Cartesian coordinate to polar coordinate using “Polar Transform” plugin in ImageJ (Figure MS6)

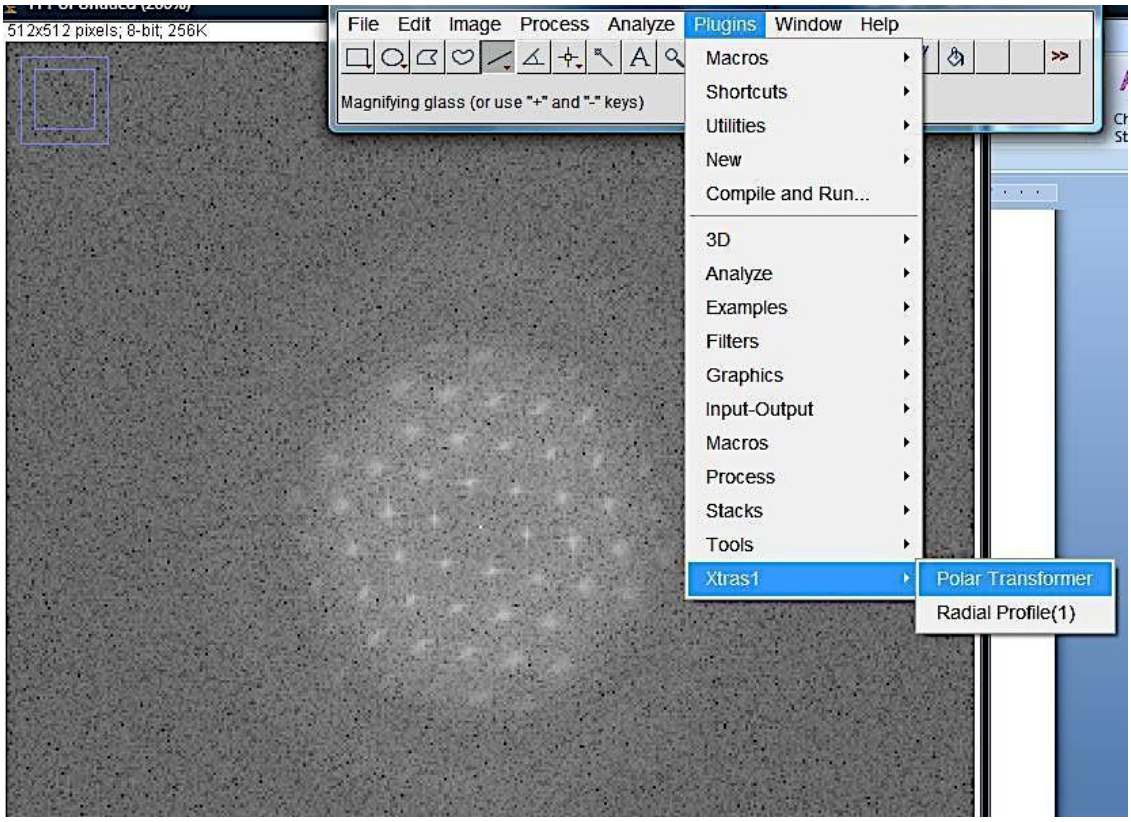

Figure MS6

A line along the (1,0) spots were drawn and intensity profile was plotted (MS7).

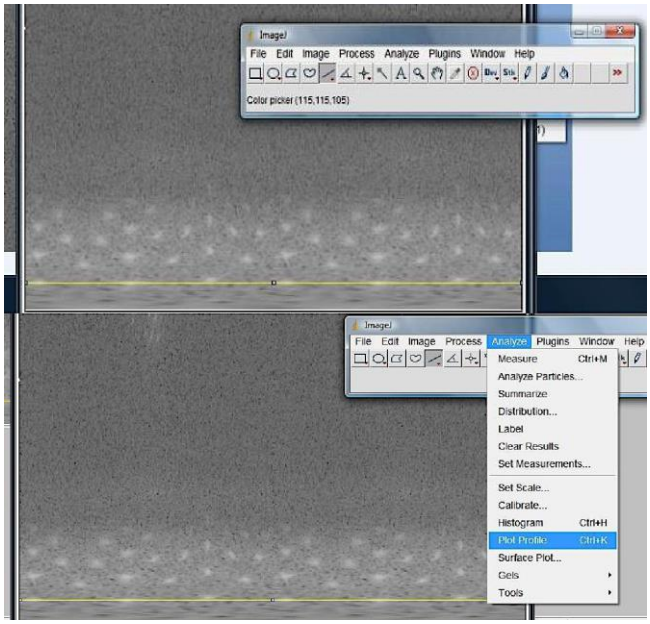

Figure MS7

From the intensity profile plot, the $\log_{10}$ of peak height of the spot intensities and the width at half maximum of the intensity peaks were measured from a baseline as shown in Figure MS8 (the double headed arrows), for each of the 6 spots in the 1,0 reflection plane and then averaged.

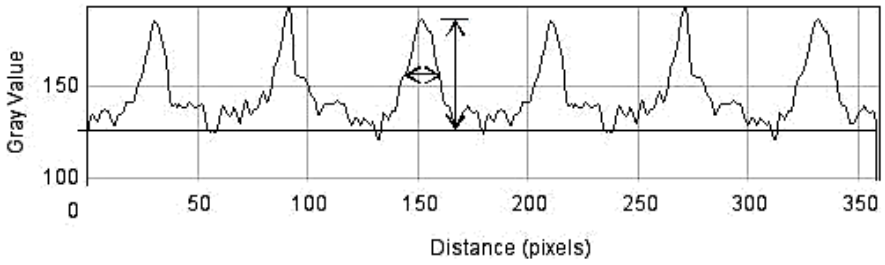

Figure MS8

The $\log_{10}$ of peak height and the width at the half maximum of the intensities are a measure of the spot sharpness and provide an estimate of the regularity of the lattice. Lower peak intensities and broader half width will indicate more variability in the spacing between lattice planes across the cross section of the myofibril.

SEP Method 8. Validation of the EM Fourier Power Spectrum Analysis to Measure Myofilament Lattice Spacing

To validate the EM Fourier power spectrum analysis to measure lattice spacing, we used the following strategies:

i) Pre-setting $d_{1,0}$ values on EM images, we measured the lattice spacing values by Fourier analysis and compared with the pre-set values.

ii) Measurement of the $d_{1,0}$ spacing values by Fourier analysis on EM images of myofibril cross-sections of the M-line region, and comparing it with that of the A-band region myofibrillar Fourier analysis.

iii) Measurement of $d_{1,0}$ values by Fourier analysis on EM images of unskinned myofibril cross-sections from flies of different ages [8] and comparing with that of the previously reported values by *in vivo* X-ray diffraction measurements [8].

iv) Pre-setting $d_{1,0}$ values on model myofibrils, we measured the lattice spacing values by Fourier analysis and compared with the pre-set values.

Validation on real myofibrillar EM images:

i) To validate if the distance between the center and the 1,0 spots in the FFT of EM myofibril images are $d_{1,0}$ spacings [9], the $d_{1,0}$ values in the *fln*$^{+}$ control cross-sectional images were pre-set in the EM images to 45nm, 50nm and 55nm. The FFT measurements were done and correlated with the pre-set values as shown below in Table MS1.

Table MS1. FFT measurement validation by pre-set $d_{1,0}$ values in the EM myofibrillar images of the control *fln*$^{+}$ strain. All values mean±SEM, number in parenthesis indicate number of image measurements carried out.

Strain	Pre-set $d_{1,0}$ (nm)	FFT inter-spot distance measured (nm)
fln^{+}	45	44.67±0.2 (30)
fln^{+}	50	49.49±0.2 (30)
fln^{+}	55	55.01±0.2 (30)

Results in Table MS1 indicates that the FFT measurements were very similar to the pre-set $d_{1,0}$ values in the images.

ii) The method was further validated on M-line regions of the *fln*$^{+}$ myofibril cross-sections (Figure MS9). The $d_{1,0}$ spacing values were 43.7±0.78 nm (5), where the value is mean±SEM and number in parenthesis indicate number of measurements performed. This value is similar to the control line $d_{1,0}$ value calculated on cross-section at the A-band region with both thick and thin filaments (compare with Table II), and are similarly ~11% smaller compared to previously reported *in vivo* values in X-ray diffraction measurements of live flies [10, 11]. This is due to lattice shrinking by dehydration steps performed for electron microcopy sample preparation ([11])

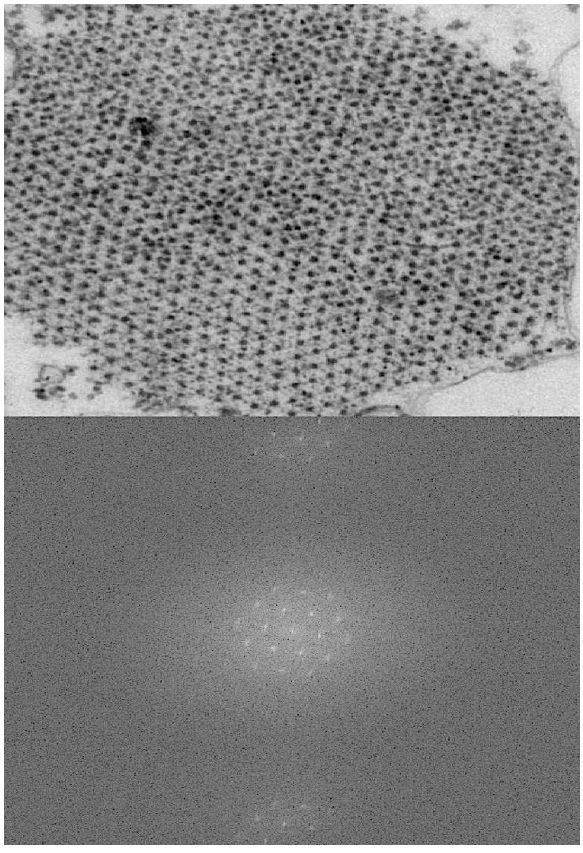

Figure MS9

iii) To further validate the FFT analysis, using the young, median aged and old fly IFM myofibrillar cross-sectional images taken by Miller MS et al. Biophys J (2008) [11], the $d_{1,0}$ spacings were measured and corresponding inter-thick filament spacings were calculated by multiplying d1,0 with $2/\sqrt{3}$. The analysis result is shown below in Table MS2.

Table MS2. FFT analysis on myofibrillar cross-sectional EM images from flies of different ages as used for *in vivo* X-ray diffraction experiments done in [11]. All values are mean±SEM, numbers in parenthesis indicate number of myofibrillar cross-sections analyzed. * $p<0.05$ vs Young and Median aged flies.

Fly age	$d_{1,0}$ (nm)	Inter-thick filament spacing (nm)	Inter-thick filament spacing of live flies (nm) [11]
Young (1-3 days)	43.51±0.3 (22)	50.24±0.43 (22)	55.63±0.12 (19)
Median (7 weeks)	42.69±0.2 (75)	49.29±0.25 (75)	55.54±0.43 (8)
Old (8 weeks)	46.84±0.51 (20)	54.08±0.60 * (20)	57.41±0.45 * (13)

The inter-thick filament spacing in our FFT measurements (Table MS2) are ~ 6-11% smaller compared to *in vivo* X-ray diffraction measurements [11] due to lattice shrinkage by dehydration steps during EM preparation. The lattice spacing in the myofibrils of old (8 weeks) flies are significantly greater compared to that of young or median aged flies (Table MS2), which is in accordance with the *in vivo* X-ray diffraction data [11]. This is a further validation of the FFT analysis for measuring $d_{1,0}$ lattice spacing.

iv) Validation on myofilament lattice models:

To validate the findings of the FFT analysis on real EM myofibrillar cross-section images, two models were created. Figure MS10 shows a model myofibril (MyAc model) with the double hexagonal lattice of thick filaments (large hollow points) and thin filaments (small filled points), and its corresponding FFT spectrum, brightness and contrast adjusted for clarity (not adjusted in real image FFTs, Table II data).

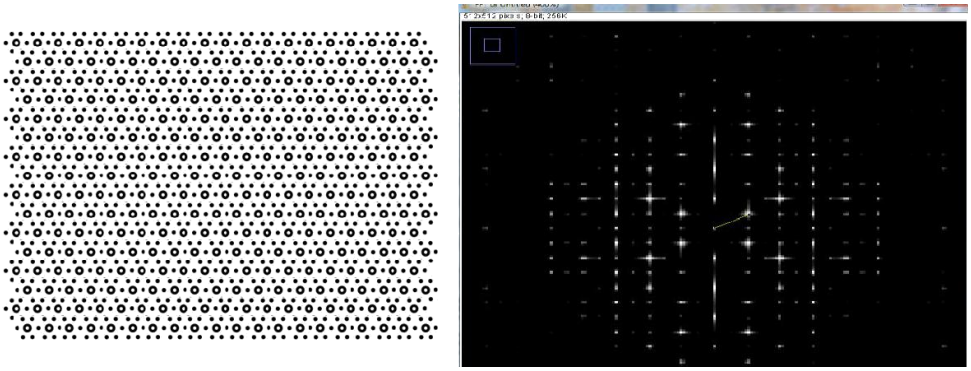

Figure MS10. Myofibril cross-section model (MyAc model) and corresponding FFT.

Figure MS11 shows a model myofibril with only the large hollow points representing the thick filaments (M model), without the thin filaments, and its corresponding FFT spectrum (brightness and contrast adjusted).

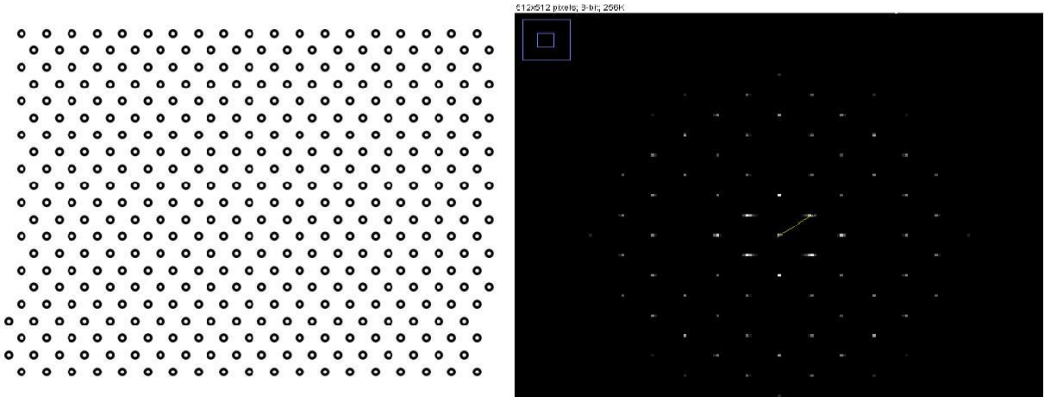

Figure MS11. Myofibril cross-section model (M model) and corresponding FFT.

The FFT spectrum of figure MS10 contains the spots from the FFT spectrum of figure MS11, which represents the myosin only lattice, and additional much weaker spots representing only the actin lattice. These weaker spots have spacings that are

approximately half those of the myosin lattice correlating well with the almost double distance in Real space. A comparison of these two lattice models with the experimental data (figure MS2) reveals that the contribution from the myosin lattice overwhelms the diffraction pattern, which shows almost no contribution from the actin lattice. A simple explanation is that the actin lattice is more disordered as can be observed by visual inspection of the micrograph shown in figure MS2.

Table MS3. FFT measurement validation by pre-set $d_{1,0}$ values on myofibillar models. All values are mean±SEM, number in parenthesis indicate number of measurements carried out.

Model	Pre-set $d_{1,0}$ (nm)	FFT inter-spot distance measured (nm)
MyAc	45	44.75±0.06 (30)
MyAc	50	49.59±0.05 (31)
MyAc	55	54.70±0.08 (30)
M	45	44.98±0.02 (30)
M	50	49.86±0.05 (31)
M	55	55.08±0.08 (30)

Table MS3 shows the FFT analyzed values for the different myofibrillar models (Figures MS10 and MS11), where the measured values are similar to the pre-set $d_{1,0}$ spacing values in each model tested. Moreover, there was no significant difference between FFT analyzed values of the myofibril models and the real myofibril cross-section of *fln*$^{+}$ control strain (compare Table MS3 vs MS1).

Overall, real and model myofibril FFT analyses using pre-set $d_{1,0}$ spacing values indicated that the FFT spots of the real myofibril cross-sections (Figure 3C and 3F) are representative of the thick filament (1,0) planar diffraction and subsequent harmonics of

it. This further indicated that the distance from the center of the Fourier space to the 1,0 reflection spots is $d_{1,0}$ spacing in the myofilament lattice real space.

SEP Method 9. Single Muscle Fiber Mechanics by Sinusoidal Analysis

Solutions for muscle fiber mechanics were prepared according to a computer program that solves the ionic equilibria [12]. Unless listed otherwise, all chemicals were purchased from Sigma-Aldrich (St. Louis, MO). Skinning solution was the same as the one used for the skinning fibers for gel electrophoresis (see SEP Method 4). Storage solution was skinning solution without Triton X-100. Concentrations are expressed in mmol/L. Activating solution was pCa 4.5, 20 BES, 20 CP, 450 U/mL CPK, 1 DTT, 5 EGTA, 1 Mg^{2+}, 12 MgATP, 2 P_i, 200 mEq ionic strength, pH 7.0. Relaxing solution was the same as activating solution except pCa adjusted to 8.0. Rigor solution was similar to activating solution without CP, CPK and MgATP. Dextran T-500 (Pharmacosmos, Holbaek, Denmark) was added to all activating, relaxing and rigor solutions to a final concentration of 4% w/v to compress the myofilament lattice spacing to near *in vivo* values [11]. Fiber preparation, mechanical measurements and curve fitting were carried out as in previous studies [10, 11] with the following modifications. Briefly, fibers from 2-3 days old flies were mounted on T-clips in the relaxing solution, then activated, and shortened until slack. After the fiber tension is stable in either relaxing or activation conditions, sinusoidal length perturbation analyses were done to retrieve elastic and viscous moduli values and oscillatory work output (in case of active condition) at each different frequency. After pausing for five minutes, fibers were re-stretched from slack to just taut to a stable tension level, and then sequentially stretched in 3% increments until oscillatory work reached a stable maximum, as measured by sinusoidal length-perturbation analysis. The mutant fibers had to be stretched further (~16%) compared to control fibers (27.8 ± 2.7 % vs 23.9 ± 1.3 % stretch for control) from initial length at just

taut. The stretched fiber was then washed into relaxing solution and stable passive tension was noted down. Finally, the fiber was placed in rigor solution and left in it for few minutes until tension rises to a stable maximum which was noted down and then sinusoidal length perturbation analysis was performed to retrieve elastic and viscous moduli in rigor condition. In each of the conditions (relax, active or rigor), the fiber was allowed to generate a stable isometric tension before performing sinusoidal length-perturbation analysis.

SEP Method 10. Transmission Electron Microscopy on Fibers Torn in Rigor

Individual skinned muscle fibers with aluminum T-clips on both ends that tore in rigor during fiber mechanics experiments were removed very quickly from the strain gauge and motor after the completion of the mechanics protocol (see SEP Method 9), and very quickly put in Karnovsky's fixative (2.5% v/v glutaraldehyde, 1% v/v paraformaldehyde in 0.1M Cacodylate buffer) to fix overnight, embedded in a small block of agarose (for ease of handling and visualizing single fibers), and prepared for imaging like the bisected fly thoraces as previously described [10]. Images were at 8000x magnification, 1.426 nm pixel size.

SEP Method 11. Statistical Analysis

All values are mean ± SE. Statistical analyses were performed using SPSS (v.20.0, SPSS, Chicago, IL) and Matlab, with values considered significant at $p<0.05$. Student's t-test was used to examine differences between fln^{+} and $fln^{\Delta N62}$ for most variables except for the elastic modulus-, viscous modulus-, work-, and power-frequency relationships. For

these measurements, we applied a linear mixed model using frequency as the repeated measure, followed by Fischer's LSD pairwise comparisons between the two groups at each frequency.

SUPPLEMENTAL RESULTS

Generation of *Drosophila* Transgenic Lines Expressing an N-terminal Truncated Flightin

Flightin is a myosin rod binding protein [17] required for normal length, structural integrity and stiffness of the IFM tick filaments [18]. To investigate the functional properties of the N-terminal region of flightin, we generated transgenic lines expressing both the endogenous flightin and a flightin construct missing amino acids 2 through 63. Five lines with independent second chromosome insertions were tested for their flight ability and wing beat frequency. All of the lines behaved similarly to full length flightin rescued control null strain, fln^{+} flies [1] indicating that the mutated transgene does not have a dominant negative effect (data not shown). We next crossed each transgenic to fln^{0} to generate lines expressing an N-terminal truncated flightin in the absence of endogenous flightin. The lines were found not to differ significantly from each other in protein expression and flight performance (data not shown). Two lines were chosen for this study and the data combined (herein referred to as $fln^{\Delta N62}$) when the muscle structural and mechanical analyses (described below) showed they did not differ from one another. The mutant flightin construct codes for a 120 amino acid protein with a predicted molecular mass of 14,381 Da, compared to 20,656 Da for the full-length flightin [13]. One dimensional SDS-PAGE (Figure S2A) and western blot analysis (Figure S2B) of proteins extracted from skinned IFM fibers from $fln^{\Delta N62}$ and fln^{+} flies show that the

truncated flightin is expressed and incorporated in the myofibril. As predicted from its theoretical molecular mass, the truncated protein migrates further (~15 kDa) than full-length flightin, which typically migrates at ~26 kDa [13]. The N-terminal truncated flightin is recognized by an anti-flightin polyclonal antibody, albeit not as strongly as the full length flightin (Figure S2B). This is not unexpected given that the truncation removed ~1/3 of the flightin sequence. The reduced intensity of the lower molecular mass of the N-terminal truncated flightin band compared to that of full length flightin band in the western blot (fln^{+} lane) is due to 34% truncation of the protein resulting in lower affinity of the antibody, but not due to lower functional expression. A flightin deficiency heterozygote mutant [*Df(3L)fln1*] [14] showing ~20% reduction in flightin expression showed much less improved myofilament organization and mechanical properties compared to $fln^{\Delta N62}$ that we report here, suggesting a fair conclusion that the N-terminal truncation of flightin does not reduce protein expression.

Table S1. Isometric Tension Measurements from Skinned IFM Fibers.

Line	Relaxed tension (kN/m^2)	Net active tension (kN/m^2)	Net rigor tension (kN/m^2)	Net rigor yield strength (kN/m^2)
fln^{+}	1.7±0.3 (15)	1.5±0.2 (15)	3.1±0.4 (11)	5.3±0.4 (2)
fln$^{\Delta N62}$	0.9±0.1* (15)	0.8±0.1* (15)	1.1±0.2* (8)	1.6±0.1* (3)

Values are mean ± SE. Numbers in parentheses indicate number of fibers analyzed. Net active (pCa4.5) and net rigor (pCa4.5) values represent tension increase from relaxed (pCa8.0) condition.

Net rigor yield strength = maximal tension withstood before fiber starts tearing minus relaxed tension.

* Significant difference ($p<0.05$) from *fln*$^{+}$ control.

Audio S1. Male courtship song (sine and pulse) sample of *fln*$^{+}$ male (Figure S3 middle panel) in the presence of a wild type (Oregon R) strain female mate.

Audio S2. Male courtship song (sine and pulse) sample of *fln*$^{\Delta N62}$ male (Figure S3 bottom panel) in the presence of a wild type (Oregon R) strain female mate.

Video S1. Male courtship success of *fln*$^{+}$ with wild type (Oregon R strain) female mate in a single pair mating assay (see Materials and Methods).

Video S2. *fln*$^{\Delta N62}$ male gets courtship success for wild type (Oregon R strain) female mate in a single pair mating assay (see Materials and Methods).

Video S3. *fln*$^{\Delta N62}$ male gets outcompeted by *fln*$^{+}$ control male for wild type (Oregon R strain) female mate choice.

SUPPLEMENTAL REFERENCES

1. Barton B., Ayer G., Heymann N., Maughan D.W., Lehmann F.O., Vigoreaux J.O. 2005 Flight muscle properties and aerodynamic performance of Drosophila expressing a flightin transgene. *J Exp Biol* **208**(Pt 3), 549-560. (doi:208/3/549 [pii] 10.1242/jeb.01425).

2. Reedy M.C., Bullard B., Vigoreaux J.O. 2000 Flightin is essential for thick filament assembly and sarcomere stability in Drosophila flight muscles. *J Cell Biol* **151**(7), 1483-1500.

3. Chakravorty S., Wajda M.P., Vigoreaux J.O. 2012 Courtship song analysis of Drosophila muscle mutants. *Methods* **56**(1), 87-94.

4. Chakravorty S., Vu H., Foelber V., Vigoreaux J.O. 2014 Mutations of the Drosophila myosin regulatory light chain affect courtship song and reduce reproductive success. *PloS one* **9**(2), e90077. (doi:10.1371/journal.pone.0090077).

5. 2010 Goldwave Inc. *St John's, Newfoundland, Canada*.

6. Schneider C.A., Rasband W.S., Eliceiri K.W. 2012 NIH Image to ImageJ: 25 years of image analysis. *Nat Methods* **9**(7), 671-675.

7. Irving T.C. 2006 X-ray diffraction of indirect flight muscle from Drosophila in vivo. . *In Nature's Versatile Engine: Insect flight Muscle Inside and Out. JO Vigoreaux, editor Landes Bioscience, Georgetown, TX*, 197-213.

8. Miller M.S., Lekkas P., Braddock J.M., Farman G.P., Ballif B.A., Irving T.C., Maughan D.W., Vigoreaux J.O. 2008 Aging enhances indirect flight muscle fiber

performance yet decreases flight ability in Drosophila. *Biophysical journal* **95**(5), 2391-2401. (doi:10.1529/biophysj.108.130005).

9. Irving T.C. 2006 X-ray diffraction of indirect flight muscle from Drosophila in vivo. *In Nature's Versatile Engine: Insect flight Muscle Inside and Out JO Vigoreaux, editor Landes Bioscience, Georgetown, TX*, 197-213.

10. Tanner B.C., Miller M.S., Miller B.M., Lekkas P., Irving T.C., Maughan D.W., Vigoreaux J.O. 2011 COOH-terminal truncation of flightin decreases myofilament lattice organization, cross-bridge binding, and power output in Drosophila indirect flight muscle. *Am J Physiol Cell Physiol* **301**(2), C383-391. (doi:10.1152/ajpcell.00016.2011 ajpcell.00016.2011 [pii]).

11. Miller M.S., Farman G.P., Braddock J.M., Soto-Adames F.N., Irving T.C., Vigoreaux J.O., Maughan D.W. 2011 Regulatory light chain phosphorylation and N-terminal extension increase cross-bridge binding and power output in Drosophila at in vivo myofilament lattice spacing. Biophysical journal 100(7), 1737-1746. (doi:10.1016/j.bpj.2011.02.028).

12. Godt R.E., Lindley B.D. 1982 Influence of temperature upon contractile activation and isometric force production in mechanically skinned muscle fibers of the frog. The Journal of general physiology 80(2), 279-297.

13. Vigoreaux J.O., Saide J.D., Valgeirsdottir K., Pardue M.L. 1993 Flightin, a novel myofibrillar protein of Drosophila stretch-activated muscles. *J Cell Biol* **121**(3), 587-598.

14. Vigoreaux J.O., Hernandez C., Moore J., Ayer G., Maughan D. 1998 A genetic deficiency that spans the flightin gene of Drosophila melanogaster affects the ultrastructure and function of the flight muscles. *J Exp Biol* **201**(Pt 13), 2033-2044.

15. Coen P., Xie M., Clemens J., Murthy M. 2016 Sensorimotor Transformations Underlying Variability in Song Intensity during Drosophila Courtship. *Neuron* **89**(3), 629-644. (doi:10.1016/j.neuron.2015.12.035).

16. Ejima A., Griffith, L.C. 2007 Measurement of courtship behavior in Drosophila melanogaster. *Cold Spring Harb Protoc*. (doi:10.1101/pdb.prot4847).

17. Ayer G., Vigoreaux J.O. 2003 Flightin is a myosin rod binding protein. *Cell Biochem Biophys* **38**(1), 41-54.

18. Contompasis J.L., Nyland L.R., Maughan D.W., Vigoreaux J.O. 2010 Flightin is necessary for length determination, structural integrity, and large bending stiffness of insect flight muscle thick filaments. *Journal of molecular biology* **395**(2), 340-348. (doi:S0022-2836(09)01398-9 [pii] 10.1016/j.jmb.2009.11.021).